AGU PUBLICATIONS

Water Resources Research

RESEARCH ARTICLE

10.1002/2017WR021701

Optimizing Multireservoir System Operating Policies Using Exogenous Hydrologic Variables

Jasson Pina[1], Amaury Tilmant[1], and Pascal Côté[2]

[1]Department of Civil Engineering and Water Engineering, Université Laval, QC, Canada, [2]Rio Tinto, Quebec Power Operation, Jonquiére, QC, Canada

Key Points:

- The SDDP algorithm can handle multiple endogenous and exogenous hydrologic state variables
- Gains in energy production can be observed when more hydrologic variables are included in the state space vector
- The marginal water values tend to increase while spillage losses are reduced regardless of the hydrologic status of the system

Correspondence to:
A. Tilmant,
amaury.tilmant@gci.ulaval.ca

Citation:
Pina, J., Tilmant, A., & Côté, P. (2017). Optimizing multireservoir system operating policies using exogenous hydrologic variables. *Water Resources Research*, *53*, 9845–9859. https://doi.org/10.1002/2017WR021701

Received 19 AUG 2017
Accepted 10 NOV 2017
Accepted article online 15 NOV 2017
Published online 28 NOV 2017

Abstract Stochastic dual dynamic programming (SDDP) is one of the few available algorithms to optimize the operating policies of large-scale hydropower systems. This paper presents a variant, called SDDPX, in which exogenous hydrologic variables, such as snow water equivalent and/or sea surface temperature, are included in the state space vector together with the traditional (endogenous) variables, i.e., past inflows. A reoptimization procedure is also proposed in which SDDPX-derived benefit-to-go functions are employed within a simulation carried out over the historical record of both the endogenous and exogenous hydrologic variables. In SDDPX, release policies are now a function of storages, past inflows, and relevant exogenous variables that potentially capture more complex hydrological processes than those found in traditional SDDP formulations. To illustrate the potential gain associated with the use of exogenous variables when operating a multireservoir system, the 3,137 MW hydropower system of Rio Tinto (RT) located in the Saguenay-Lac-St-Jean River Basin in Quebec (Canada) is used as a case study. The performance of the system is assessed for various combinations of hydrologic state variables, ranging from the simple lag-one autoregressive model to more complex formulations involving past inflows, snow water equivalent, and winter precipitation.

1. Introduction

The operation of a multireservoir system is a complex, multistage, stochastic decision-making problem involving, among others, (i) a trade-off between immediate and future consequences of a release decision, (ii) considerable risks and uncertainties, and (iii) multiple objectives and operational constraints (Oliveira & Loucks, 1997). For hydropower systems, the problem can also be nonlinear because the production of hydroelectricity depends on the product of the outflow and the head (storage). This decision-making problem has been studied for several decades and state-of-the-art reviews can be found in Yeh (1985), Labadie (2004), Rani and Moreira (2009)], and more recently in Ahmad et al. (2014).

Dynamic programming (DP), first introduced by Bellman (1957), has been one of the most popular optimization techniques to determine reservoir operating policies. The method solves the problem by decomposing the multistage decision-making problem into simpler one-stage problems, which are then solved recursively. DP can be easily expanded to accommodate the stochasticity of the hydrologic input by adding a hydrologic variable to the state space vector. The resulting stochastic DP (SDP) formulation, often referred to as a Markov decision process, explicitly considers the streamflow lag-1 correlation found in the flow records. SDP solves the problem by discretizing stochastic variables, as well as the system status, to obtain an optimal solution for each discrete value of the state space that characterizes the system (Tejada-Guibert et al., 1995). Although conceptually attractive, SDP is however limited by the so-called curse of dimensionality, which limits its application to small systems involving no more than four state variables (storage and hydrologic).

Incorporating more hydrologic information in the state vector has the potential to enhance SDP-derived policies and thus improve the performance of the system. Various approaches have been proposed the literature to address this challenge. For example, Bras et al. (1983) combine real time forecasts with an adaptive control technique in SDP to update flow transition probabilities. Stedinger et al. (1984) develop an SDP model which employs the best inflow forecast for the current period's flow to define the policy. Kelman et al. (1990) propose sampling SDP (SSDP) to better capture the complex temporal and spatial structures of the streamflow process. Karamouz and Vasiliadis (1992) propose another alternative to SDP, coined Bayesian SDP (BSDP), in which prior flow transition probabilities are regularly updated using the Bayes' theorem. Tejada-Guibert et al. (1995) determine the value of hydrological information for several SDP formulations each employing a different set of hydrologic state variables and, similarly, Kim and Palmer (1997) illustrate the potential advantage of using the seasonal flow forecasts and other hydrologic information by comparing the performance of the BSDP against alternative SDP formulations. Furthermore, Faber and Stedinger (2001) and Kim et al. (2007) examine the use Ensemble Streamflow Prediction (ESP) within the SSDP optimization framework. Côté et al. (2011) incorporate a new hydrologic state variable in SSDP as a linear combination of snow water equivalent and soil moisture, and more recently, Desreumaux et al. (2014) present the effect of using various hydrological variables on SDP-derived policies of the Kemano hydropower system in British Columbia. Another active research line focuses on the incorporation of climate variables such as the El Nino Southern Oscillation (ENSO) and Pacific Decadal Oscillation (PDO) climate signals into reservoir operation models (Gelati et al., 2013; Hamlet & Lettenmaier, 1999; Kwon et al., 2009). However, most of the above-mentioned studies are limited to small-scale problems, meaning that a trade-off must be found between the complexity of system to be studied (number of reservoirs) and the complexity of the hydrologic processes that can be captured.

This trade-off between system and hydrologic complexities can largely be removed using stochastic dual DP (SDDP), an extension of SDP that is not affected by the curse of dimensionality (Pereira & Pinto, 1991). To achieve this, SDDP builds a locally accurate approximation of the expected-benefit-to-go functions through piecewise linear functions. With such an approximation, there is no need to evaluate the function over a dense grid; the benefits can now be derived from extrapolation and not interpolation as in SDP. As we will see later, these piecewise linear functions are constructed from the primal and dual solutions of the one-stage optimization problem and can be interpreted as Benders cuts in a stochastic, multistage decomposition algorithm. To increase the accuracy of the approximation, SDDP uses an iterative procedure in which new cuts are added to the most interesting region of the state space until the approximation is statistically acceptable. As explained in Tilmant and Kelman (2007), to implement the decomposition scheme, the one-stage optimization problem must be formulated as a convex problem, such as a linear program. SDDP has largely been used in hydropower-dominated systems such as Norway (Gjelsvik et al., 2010; Mo et al., 2001; Rotting & Gjelsvik, 1992), South and Central America (Homen-de Mello et al., 2011; Pereira, 1989; Shapiro et al., 2013), and New Zealand (Kristiansen, 2004). The SDDP algorithm constitutes the core of generic hydro-economic models that have been used to analyze a variety of policy issues in the Euphrates-Tigris River basin (Tilmant et al., 2008), the Nile River basin (Goor et al., 2011), the Zambezi River basin (Tilmant & Kinzelbach, 2012), or in Spain (Macian-Sorribes et al., 2016; Pereira-Cardenal et al., 2016).

In SDDP, the hydrologic uncertainty is typically captured through a multisite periodic autoregressive model MPAR(p). This model is capable of representing seasonality, serial, and spatial streamflow correlations within a river basin and among different basins. It is also needed to analytically derive some of the parameters of the linear segments used to approximate the benefit-to-go functions, and to produce synthetic streamflows scenarios for the simulation phase of this iterative algorithm. Furthermore, the convexity requirement of SDDP is guaranteed because the MPAR(p) is linear. Recent works reveal an interest in improving the built-in hydrological model. In Lohmann et al. (2015), a new approach to include spatial information is presented. Pritchard (2015) models inflows as a continuous process with a discrete random innovation. Poorsepahy-Samian et al. (2016) propose a methodology to estimate the cuts parameters when a Box-Cox transformation is used to normalize inflows, and more recently, Raso et al. (2017) present a streamflow model with a multiplicative stochastic component and a nonuniform time step.

This study focuses on the incorporation of new hydrologic information into the SDDP algorithm. This new information, encapsulated as additional, exogenous, hydrologic state variables through a built-in MPARX model, aims at better capturing the hydrologic processes responsible for reservoir inflows. By definition, reservoir inflows (the endogenous variables) are causal dependent on the exogenous hydrologic state variables while the opposite is not true. For example, winter snow pack, precipitation, or sea surface temperature are exogenous to river discharges. Incorporating exogenous hydrologic state variables into SDDP requires that some aspects of the iterative algorithm be modified. Particular attention is devoted to the new mathematical formulation of the cuts approximating the benefit-to-go functions, and how the corresponding parameters can be analytically derived from the primal and dual information that become available as the algorithm progresses backward (backward optimization phase). In the forward simulation phase, due to the structure of the built-in hydrologic model (MPARX), the number of hydrologic sequences is now limited to the length of hydrological records/direct measurements.

Following the temporal decomposition approach Zahraie and Karamouz (2004), the proposed SDDPX formulation solves the midterm hydropower scheduling problem and therefore seek to properly capture the midterm to long-term hydrologic uncertainties. Since the nonlinear nonconvex hydropower function cannot be used as such in the SDDP algorithm, usually simplifications of the function are used. We can rely, for example, on a production coefficient (Archibald et al., 1999), convex hull approximations (Goor et al., 2011), McCormick envelopes (Cerisola et al., 2012), or a concave approximation (Zhao et al., 2014). To deal with the nonconvexity of the optimization problem, the hydropower production functions are approximated by convex hulls. This new formulation is illustrated with the 3,137 MW hydropower system of Rio Tinto (RT) located in the Saguenay-Lac-St-Jean River Basin in Quebec (Canada). The five hydropower plants have the capacity to produce approximately 90% of the electricity required for the production of aluminum, forcing RT to purchase energy to fully ensure the production of the mineral. Therefore, a joint optimization of physical (power plants) and financial (contracts) assets is developed using SDDPX, and a comparative analysis of the performance of the system with various combinations of endogenous and exogenous hydrologic state variables is performed.

The paper is organized as follows: section 2 starts with a presentation of the reservoir operation problem, which is then followed by a description of the SDDP algorithm and its variant SDDPX with exogenous hydrologic variables. This section ends with a presentation of the case study. Afterward, optimization results are discussed in section 3. Finally, concluding remarks are given in section 4.

2. Materials and Methods

2.1. The Hydroelectric Reservoir Operation Problem

The operation of a multireservoir system is a multistage decision-making problem. When framed as an optimization problem, the goal is to determine a sequence of optimal decisions x_t that maximizes the expected sum of net benefits from system operation Z over a given planning period. Let T be the number of stages in the planning period, $b_t(\cdot)$ be the net benefit function at stage t, $v(\cdot)$ be the terminal value function, $E[\cdot]$ be the expectation operator, and S_t be a vector of state variables characterizing the system at the beginning of stage t, the objective function can be written as:

$$Z=E\left[\sum_{t=1}^{T} b_t(S_t,x_t)+v(S_{T+1})\right] \quad (1)$$

This objective function will be maximized to the extent made possible by operational and/or institutional constraints affecting the state and decision variables.

2.2. One-Stage SDDP Problem

SDDP solves the optimization problem (1) by decomposing it into a sequence of one-stage problems that are solved recursively. Let us first adopt the same notation as in Tilmant et al. (2008) and say that the water resources system is represented by a network with J nodes (e.g., reservoir, power plant). Imagine that the objective is to maximize the net benefits associated to the production of hydroelectricity. The immediate benefit function $b_t(\cdot)$ includes the net benefits from hydropower generation and penalties for not meeting target demands and/or violating constraints is expressed as

$$b_t(S_t,x_t)=\sum_{j=1}^{J}\left[P_{sys,t}(j)\tau_t(\pi_t(j)-\theta_t(j))\right]-\xi_t' z_t \quad (2)$$

where τ_t is the number of hours in period t, $P_{sys,t}$ is the vector of power generated (MW), π is the vector of energy price ($/MWh), θ is the vector of the operation and maintenance cost ($/MWh), and z_t is the vector of deficits or surpluses (e.g., energy demand, environmental flows) penalized by the vector ξ_t' of penalties ($/unit). Sales and purchases are included in vector z_t and the penalty is the price of energy specified in the corresponding contract ($/MWh).

At stage t, the system status S_t is described by the vector of storage s_t, the hydrological state variable h_t, and the amount left of energy w_t in C contracts. The one-stage SDDP optimization problem is expressed as:

$$F_t(s_t, h_t, w_t) = \max\{b_t(s_t, h_t, w_t, x_t) + F_{t+1}\} \tag{3}$$

In SDDP, the benefit-to-go function is represented by the scalar F_{t+1} which is bounded by a locally accurate linear approximation. The stage to stage transformation function corresponds to the mass balance equation involving the vector of spillage losses l_t, the vector of inflows q_t, the vector of the turbined outflows r_t, the vector of evaporation losses e_t, and the connectivity matrix CM_R

$$s_{t+1} - CM_R(r_t + l_t) = s_t + q_t - e_t(s_t) \tag{4}$$

$CM_R(j,k) = 1(-1)$ when reservoir j receives(releases) water from(to) reservoir k.

As mentioned earlier, the benefit-to-go function F_{t+1}, which is represented by a scalar in equation (3), is bounded from above by inequality constraints:

$$\begin{cases} F_{t+1} - \varphi_{t+1}^{l} s_{t+1} - \chi_{t+1}^{l} w_{t+1} & \leq & \Gamma_{t+1}^{l} h_{t+1} + \beta_{t+1}^{l} \\ & \vdots & \\ F_{t+1} - \varphi_{t+1}^{L} s_{t+1} - \chi_{t+1}^{L} w_{t+1} & \leq & \Gamma_{t+1}^{L} h_{t+1} + \beta_{t+1}^{L} \end{cases} \tag{5}$$

where L is the number of cuts. The parameters φ_{t+1}, χ_{t+1}, β_{t+1}, and Γ_{t+1} must have been calculated from the primal and the dual information available at the optimal solution of the one-stage optimization problem at the stage $t+1$ (Tilmant et al., 2008). In previous SDDP application to water resources systems, the hydrological variables are the natural inflows observed during the last p periods $h_t(j) = [q_{t-1}(j), q_{t-2}(j), \ldots, q_{t-p}(j)]$ and the current inflow is described by a multisite periodic autoregressive model MPAR(p):

$$\frac{q_t(j) - \mu_{q_t}(j)}{\sigma_{q_t}(j)} = \sum_{i=1}^{p} \phi_{i,t}(j) \left(\frac{q_{t-i}(j) - \mu_{q_{t-i}}(j)}{\sigma_{q_{t-i}}(j)} \right) + \epsilon_{\mathbf{t}}(j) \tag{6}$$

where μ_{q_t} and σ_{q_t} are, respectively, the vectors of periodic mean and standard deviation of q_t at period t, $\phi_{i,t}$ is the vector of autoregressive coefficients, and $\epsilon_{\mathbf{t}}$ is the time dependent and spatially correlated stochastic noise of zero mean and variance $\sigma_{\epsilon,t}^2$.

The nonlinear hydropower production $P_{sys,t}$ (MW), defined as the product of the net head h_t (m), the release r_t (m^3/s), the turbines/generators efficiency η, and the specific weight of water γ_w (MN/m^3):

$$P_{sys,t} = \gamma_w \cdot \eta(s_t, s_{t+1}, r_t) \cdot h(s_t, s_{t+1}) \cdot r_t \tag{7}$$

is approximated by convex hulls and stored in the constraints set (8):

$$\begin{cases} \hat{P}_{sys,t} - \psi^1 s_{t+1}/2 - \omega^1 r_t & \leq & \psi^1 s_t/2 + \delta^1 \\ & \vdots & \\ \hat{P}_{sys,t} - \psi^H s_{t+1}/2 - \omega^H r_t & \leq & \psi^H s_t/2 + \delta^H \end{cases} \tag{8}$$

where $\hat{P}_{sys,t}$ is the approximated power, H is the number of linear segments, ψ, ω, and δ are the vectors of parameters determined according to the procedure described in Goor et al. (2011).

The load D_t (MWh) must be met with the energy produced by the system $\hat{P}_{sys,t}$ and the sales/purchases through the contracts:

$$\sum_J \hat{P}_{sys,t}(j)\tau_t + \sum_C u_t(c) + P_{p,t}\Delta t - P_{s,t}\Delta t = D_t \tag{9}$$

Energy transactions can be handled by (i) instant power contracts in which a given amount of power $P_{p,t}$ can be bought and surpluses be sold $P_{s,t}$ during time period Δt, and (ii) purchase energy contracts $w_t(c)$. In the latter, the amount of energy $u_t(c) = P_{w,t}\tau_t$ that can be withdrawn from the contracts follows the energy balance equation:

$$w_{t+1}(c)+u_t(c)=w_t(c) \tag{10}$$

and it is limited by the minimum and maximum instant power withdrawn $P_{w,t}$

$$P_w^{\min}\tau_t \le u_t \le P_w^{\max}\tau_t \tag{11}$$

2.3. Incorporating Exogenous Hydrologic Variables into SDDP

Incorporating exogenous hydrologic variables into the state space vector of SDDP offers the potential to improve the performance of SDDP-derived release policies. Using p previous inflows q_t and b past exogenous variables X_t, the hydrological state variable h_t becomes $h_t=[q_{t-1}, q_{t-2},\ldots,q_{t-p}, X_{t-\kappa},\ldots, X_{t-b}]$. With these variables, the incremental flow at node j, $q_t(j)$, can be derived from a multisite periodic autoregressive model with exogenous variables MPARX(p,b) (Ljung, 1999):

$$\frac{q_t(j)-\mu_{q_t}(j)}{\sigma_{q_t}(j)}=\sum_{i=1}^{p}\phi_{i,t}(j)\left(\frac{q_{t-i}(j)-\mu_{q_{t-i}}(j)}{\sigma_{q_{t-i}}(j)}\right)+\sum_{\kappa=\imath}^{b}\vartheta_{\kappa,t}(j)\left(\frac{X_{t-\kappa}(j)-\mu_{X_{t-\kappa}}(j)}{\sigma_{X_{t-\kappa}}(j)}\right)+\epsilon_{\mathbf{t}}(j) \tag{12}$$

where μ_{X_t} and σ_{X_t} are, respectively, the vectors of the periodic mean and the standard deviation of the exogenous variables and $\vartheta_{\kappa,t}$ is the vector of the exogenous regressors. As indicated in equation (12), the exogenous variables may cover a different range of past input values, from $\imath$ to b, not necessarily starting from $t-1$.

The main modification to the traditional SDDP formulation lies in the calculation of the hyperplanes' parameters φ_{t+1}, χ_{t+1}, β_{t+1}, and Γ_{t+1} (see equation (5)). In particular, Γ_{t+1} is the vector of linear parameters $[\gamma_{t+1,1}, \gamma_{t+1,2},\ldots, \gamma_{t+1,p}, \gamma_{t+1,p+\kappa},\ldots, \gamma_{t+1,p+b}]$ associated to $h_{t+1}=[q_t, q_{t-1},\ldots,q_{(t-p)+1}, X_{(t-\kappa)+1},\ldots, X_{(t-b)+1}]$. The procedure to analytically derive the hyperplanes' parameters when exogenous hydrologic variables are added to the state space vector is described in Appendix A. This procedure is implemented in the backward optimization phase of the SDDP algorithm. The accuracy of the piecewise linear approximation of F_{t+1} is then evaluated in a forward simulation phase and if they fail to pass the test, a new backward optimization phase is implemented (otherwise the algorithm stops). At each iteration, new hyperplanes are added to the constraints set, refining the approximation of F_{t+1}.

Both phases require different sets of inflows. In the backward phase, K inflows scenarios (backward openings) at each node of the system are generated using the MPARX(p,b). Actually, as explained in Appendix A, these scenarios are needed to analytically calculate the hyperplanes' parameters, and ultimately to derive the upper bound to the true expected benefit-to-go function. In the forward phase, two different options exist to generate the M hydrologic sequences required to simulate the system: (i) one can use the MPARX(p,b) to generate synthetic streamflow sequences based on historical records of both endogenous and exogenous hydrologic variables, (ii) or one can rather rely on series generated outside of SDDPX using any relevant hydrologic model. Hence, in contrast to the MPAR model used in SDDP, the built-in hydrologic model (MPARX) can no longer be used to generate any number of streamflow sequences because the exogenous variables are independent from river discharges. This might become a limitation if limited hydrologic data are available.

2.4. Case Study

The hydroelectric system of Rio Tinto located in the Saguenay-Lac-Saint Jean River Basin, Quebec (Canada) is used as a case study. It includes four reservoirs and five hydropower plants: three on the Péribonca River and two on the Saguenay River. The drainage area is about 78,000 km^2. In the northern part of the basin, there are two large reservoirs: Manouane and Passes-Dangereuses with a storage capacity of 2.7 and 5.2 km^3, respectively. The downstream reservoir system, in which the reservoir Lac-Saint-Jean is included, drains the Basins of the Péribonka River, Ashuapmushuan River, Mistassini River, and Mistassibi River. Reservoir Lac-St-jean has important recreational and sport-fishing industries which highly constrain the storage levels during summer and autumn seasons. Figure 1 shows the reservoir system configuration of the RT hydroelectric network and Table 1 lists the main characteristics of the system.

These installations can generate more than 17 TWh/yr, which is roughly 90% of the electricity required for the production of aluminum, forcing RT to buy energy to fully ensure the production of the mineral. There are two contracts ($C=2$): one yearly energy contract and one contract available at the end of the winter season.

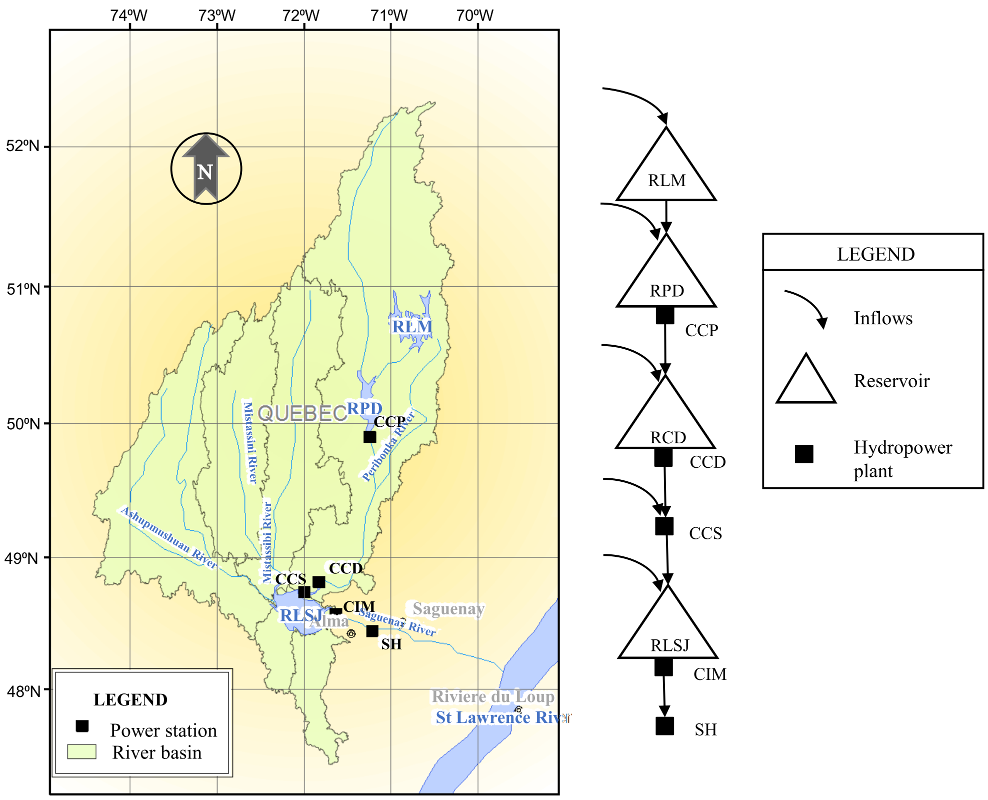

Figure 1. Rio Tinto hydropower system.

The 53 year hydrologic and climatic series (at nodes 1–5) provided by the Quebec Power Operation Department of RT are used to parameterize the multisite periodic autoregressive model with exogenous variables MPARX(*p*,*b*) (equation (12)), which residuals ϵ_t are fitted to a three-parameter log normal distribution. For this comparative analysis, four SDDP formulations, each having a specific hydrologic model, are implemented and their performance compared. The first formulation relies on a MPAR(1) model as presented in Tilmant et al. (2008). The second formulation attempts at better capturing the temporal persistence of the hydrologic processes through a MPAR(*p*) model (Matos & Finardi, 2012; Pina et al., 2016). Note that the order *p* of the autoregressive model varies in space (node) and time (week). The third and fourth formulations are based on the MPARX(*p*,*b*) described above, but differ in the selected exogenous variables, which are, respectively, the snow water equivalent SWE_t and the combination of the SWE_t and the accumulated winter precipitation P_t^w, i.e., winter precipitation from October until time *t* (Kim & Palmer, 1997). Table 2 lists the main characteristics of the alternative SDDP formulations.

Table 1
Rio Tinto Hydropower System Characteristics

Node	Id	Name	Storage (hm^3)	Capacity (MW)
1	RLM	Reservoir Lac-Manouane	2,657	
2	RPD	Reservoir Passes-Dangereuses	5,228	844
3	RCD	Reservoir Chute du Diable	396	235
4	CCS	Chute-à-la-Savane	ROR[a]	250
5	RLSJ	Reservoir Lac-St-Jean	5,083	454
6	SH	Shipshaw	ROR	1,354

[a]ROR: run of the river power plant.

Table 2
SDDP Formulations

	MPARX(*p*,*b*)		
Formulation	*p*	*b*	*X*
SDDP(1)	1		
SDDP(*p*)	*p*		
SDDPX(*p*, *SWE*)	*p*	1	*SWE*
SDDPX(*p*, *SWE*, P^w)	*p*	1	*SWE*, P^w

3. Analysis of Simulation Results

All SDDP formulations are implemented on exactly the same hydroclimatic data: $K=40$ backward openings, $M=40$ hydrological and climatic sequences over a planning period of 260 weeks ($T=260$ or 5 years). The results are analyzed after reoptimizing the polices along the 53 year historical hydrologic sequences. To achieve this, the weekly SDDP-derived benefit-to-go functions of the third year (F_{t+1}; $t=105, 106, \ldots, 157$) are used to determine the corresponding release decisions by maximizing current plus expected future benefits, subject to system constraints. Retrieving the cuts of the third year is motivated by the fact that the impacts of the boundary conditions (initial storages and zero terminal value functions) on the benefit-to-go functions are minimal when a time period of 2 years is used as a buffer zone (years 1 and 2 for the initial conditions and years 4 and 5 for the terminal conditions). When dealing with systems with larger carry-over storage capacity, it might be needed to increase the length of the buffer zone by increasing the length of the planning period (e.g., from 5 to 10 years).

To better perceive the advantage of incorporating more hydrologic state variables, the problem is solved for two different configurations based on the RT power system. The first system configuration is a simplified, hypothetical, system with a single objective: the maximization of hydropower generation. Important secondary objectives like recreation and flood control as well as the energy load and the contracts are ignored in order to dedicate all the flexibility offered by the reservoirs to the production of energy. These secondary objectives are included in the second configuration which is the actual model of the system. Here the optimization is performed on both the physical (power plants, reservoirs) and financial assets (portfolio of contracts).

Using SDDP(1) as a benchmark, Table 3 lists, for both configurations, the mean annual reduction in spillage losses and the annual energy gains one can expect when more hydrologic state variables (endogenous and exogenous) are added to the state space vector. For the second configuration, Table 3 also shows the reduction in energy purchases.

3.1. Maximization of Hydropower Generation

As we can see in Table 3, increasing the number of lags from 1 to *p* in the first configuration already increases the amount of energy produced by 54.41 GWh. Incorporating exogenous variables further increases the production of energy by 46.3 and 50.9 GWh depending on whether *SWE* or the combination of *SWE* and winter precipitation are used. Assuming an average market price of 45 US$/MWh (New York Independent System Operator, 2017), these gains correspond to a 2.45–4.70 million US$ increase in annual energy value. These energy gains are made possible by improved operating policies that better exploit the storage capacity of the system.

Figure 2 presents the drawdown-refill cycle of the two largest reservoirs of the system, Passes-Dangereuses Reservoir (RPD) and Lac-St-Jean Reservoir (RLSJ). The simulated trajectories reveal how the incorporation of the exogenous hydrologic variables affects the operating policies during the winter, and the extent to which the reservoirs must be depleted before the spring snowmelt. In this power system, a large portion of the energy comes from run-of-river power stations that are prone to spilling. Consequently, lowering the

Table 3
Average Annual Results-Differences With Respect to the SDDP(1) Model

	First configuration		Second configuration		
Model	Spillage reduction (m^3/s)	Annual gain of energy (GWh)	Spillage reduction (m^3/s)	Annual gain of energy (GWh)	Net purchases reduction (%)
SDDP(*p*)	15	54	10	30	4.0
SDDPX(*p*, *SWE*)	35	101	26	50	6.6
SDDPX(*p*, *SWE*, P^w)	33	105	28	51	6.7

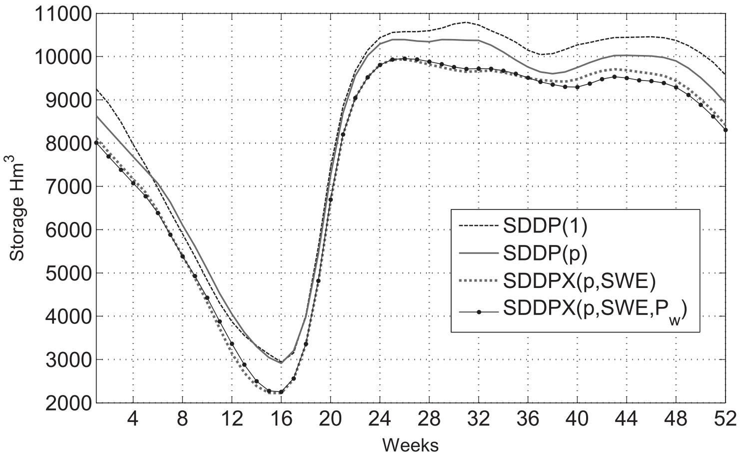

Figure 2. Weekly mean storage at reservoirs Passes-Dangereuses (RPD) and Lac-St-Jean (RLSJ). First configuration.

storage levels in the upstream reservoirs tend to reduce the spillage losses throughout the system, therefore increasing the total energy output and compensating for the reduced efficiency at the storage power plants. With better forecasts throughout the system, the upstream reservoirs are operated at lower pool elevation to prevent excessive spills not only at the reservoir site, but also downstream.

Since the decisions taken during the drawdown phase have consequences beyond the summer, Figure 3 also explores the statistical distribution of the storage decisions for weeks 14, 15, and 16, when storage levels are the lowest. In week 14, for example, when the simple SDDP(1) and SDDP(p) formulations are used, the volume in storage exceeds 2 km^3 100% of the time. However, when the exogenous variables are included in the algorithm, storage volumes exceed this capacity less than 40% of the time, meaning that 6 years out of 10, the storage levels in week 14 will be lower than 2 km^3. These results clearly indicate that the incorporation of exogenous variables yields policies that better anticipates snowmelt runoff, therefore avoiding massive spills.

The impact of these decisions on the amount of water spilled is further analyzed in Figure 4 where we can see the probability distributions of annual spillages (left plots) at each power plant for two SDDP formulations: the simple SDDP(1) and the more sophisticated SDDPX(p, SWE, P^w). With SDDPX, the spills are reduced regardless of the hydrologic conditions, and the reduction is more pronounced in RLSJ, the downstream reservoir supplying the two largest power stations accounting for about two-thirds of the installed

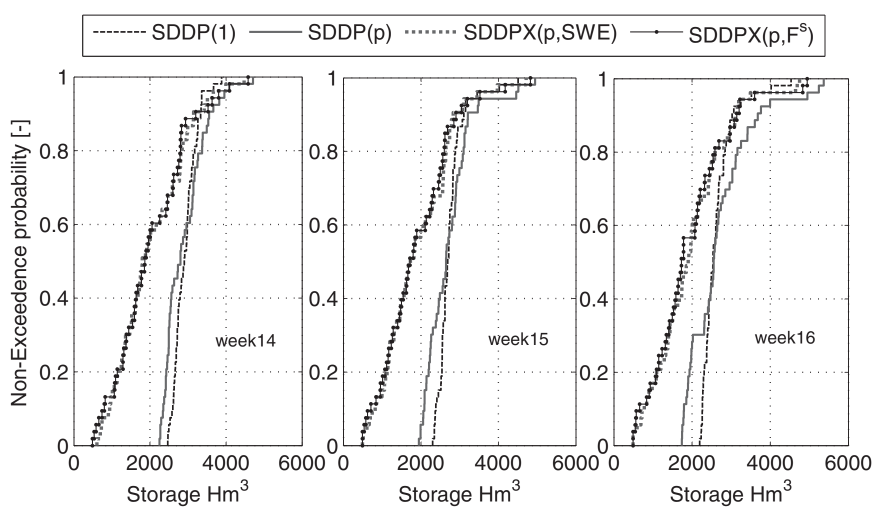

Figure 3. Statistical distribution of the accumulated storages for the largest reservoirs for weeks 14, 15, and 16. First configuration.

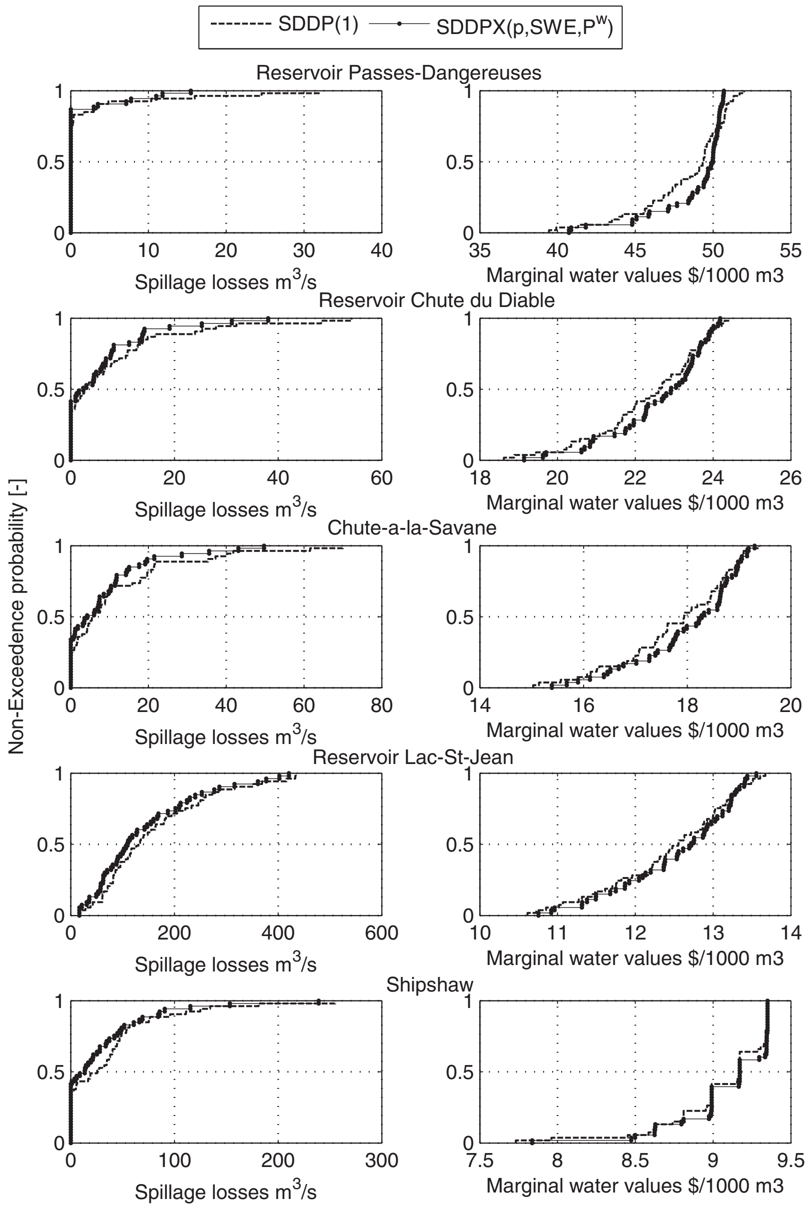

Figure 4. Statistical distributions of (left) spillage losses and (right) marginal water values. First configuration.

capacity. During dry years, however, the differences between the statistical distributions become marginal because the SDDP formulations with and without exogenous variables generate similar policies (from a decision-making point-of-view, the exogenous variables become informationless). For the most upstream reservoir (RPD), the large storage to inflow ratio implies that this reservoir does not spill 3 years out of 4. When spills do occur, SDDPX release decisions significantly reduce the discharges through the spillway, therefore having a positive repercussion on downstream infrastructure: the smaller reservoir (RCD) and the run-of-river power plant (CCS).

The exogenous hydrologic state variables also have an impact on the marginal water values, which correspond to the Lagrange multipliers associated with the mass balance equation (4). Figure 4 (right plots) compares the statistical distributions of the marginal water values in the system with the SDDP(1) and SDDPX(p, SWE, P^w) formulations only (for clarity, the two intermediate formulations are not shown). As we can see, SDDPX-derived policies yield larger water values across a wide range of hydrologic conditions. At

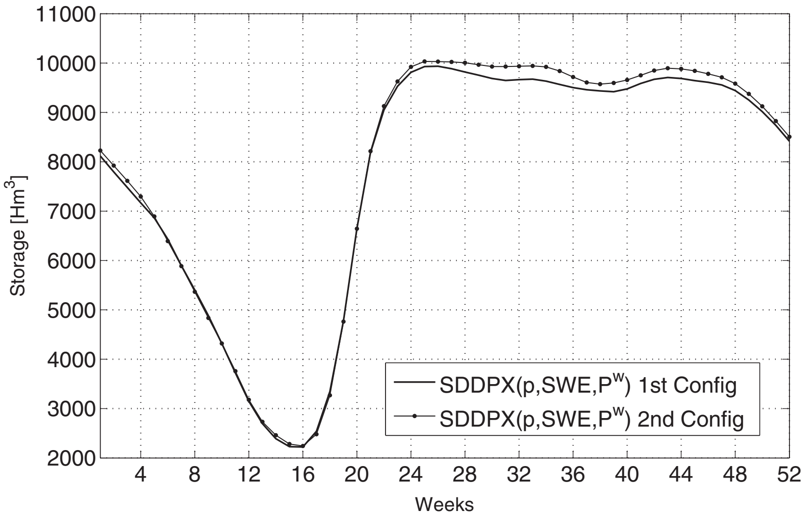

Figure 5. Average weekly storages at reservoirs Passes-Dangereuses (RPD) and Lac-St-Jean (RLSJ)-Formulation SDDPX(p,SWE,P^w) for both configurations.

any given power plant, reservoir operators would therefore be willing to pay more for the same unit of water under SDDPX release policies because, as explained above, unproductive spills are reduced.

3.2. Joint Optimization of Physical and Financial Assets

Let us now move to the second configuration. Incorporating the secondary operating objectives (recreation and flood control in Lac-Saint-Jean Reservoir) and the load commitment reveals one main change with respect to the first configuration: the gains in energy generation that we can expect with the SDDP(*p*) and SDDPX formulations are reduced (Table 3). With the most complex SDDPX formulation, the average annual gain is about 105 GWh in the first configuration. In the second configuration, the annual gain is reduced to 51 GWh. It turns out that by constraining the system and forcing the operators to buy increasingly more expensive energy to meet the load, the resulting SDDPX decisions tend to hedge more against the hydrological risk: the operating policies tend to store more water, accepting immediate, shorter, energy deficits to reduce the probability of greater, increasingly more costly, energy shortages in the future. Figure 5 shows the average weekly storages associated to the most complex SDDPX formulation for both configurations. As discussed earlier, the higher storage levels in the second, more restrictive, configuration tend to increase the unproductive spills throughout the system, therefore affecting the total energy output.

Compared to SDDP(1), the reduction in power output is however less important with SDDPX-derived policies; the net energy purchases (i.e., differences between purchases and sales) are reduced by 6.6% and 6.7% when the exogenous variables are included (Table 3).

The results can also be analyzed in terms of the annual power efficiency of the system, which is defined here as the ratio between the power produced by the system and the total outflow. Generally speaking, the average efficiency is improved when more hydrologic variables are incorporated in the state space vector (see Table 4). We can see that the power efficiency of the system actually increases when the storage levels in the head reservoir are lowered. This apparently counter-intuitive result is due to the characteristics of the RT cascade where a significant portion of the energy is generated by downstream run-of-river power plants that are prone to large spills especially if the head reservoir is also spilling. In a cascade with storage power plants, the conclusions would probably be different: power efficiency would increase with the storage levels.

Table 4
Average Power Efficiency of the System

	Average efficiency (MW/m^3 s^{-1})	
	First configuration	Second configuration
SDDP(1)	1.3976	1.3997
SDDP(*p*)	1.4019	1.4014
SDDPX(*p*, *SWE*)	1.4056	1.4033
SDDPX(*p*, *SWE*, P^w)	1.4060	1.4034

Figure 6 shows, for both configurations, the statistical distributions of the annual differences in power efficiency between SDDPX(p, SWE, P^w) and SDDP(1) formulations. As we can see, the system's efficiency is

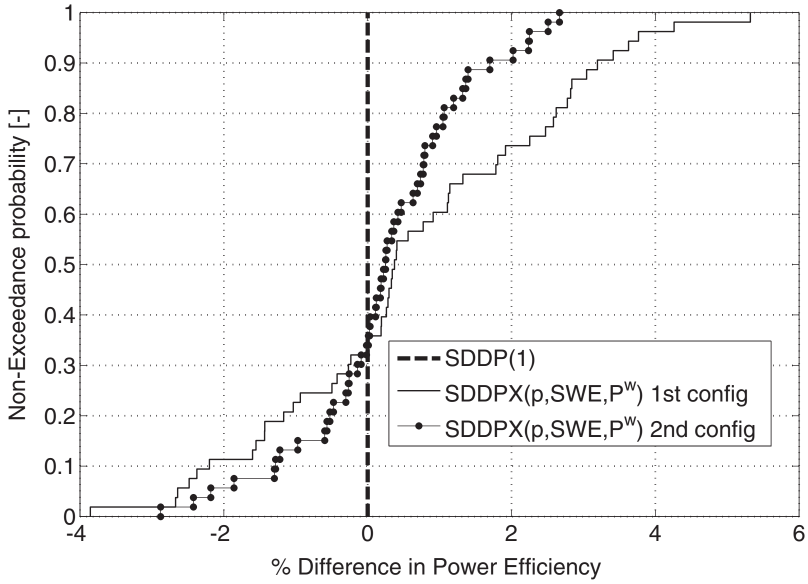

Figure 6. % of difference in the power efficiency with respect to SDDP(1) formulation for both configurations.

enhanced more than 65% of the time (the nonexceedance probability > 0.35) when the exogenous hydrologic variables are taken into account. During the rest of the time, failed inflow forecasts lead to ill-informed decisions which affect the overall efficiency of the system in the following months. Of interest is the fact that the variability of the efficiency gains/losses is less pronounced for the second configuration. In that case, both the upside and the downside of the hydrological risk associated with imperfect forecasts are partly suppressed. As energy shortages are increasingly costly, i.e., compensated by purchases through increasingly more expensive contracts, the SDDPX release policies acts as a hedging mechanism thereby yielding more conservative release decisions over the entire spectrum of the hydrologic uncertainty.

4. Discussion and Conclusions

As the availability of various hydroclimatic information keeps increasing due to advances in environmental monitoring systems, there is a need for decision-making processes and tools that can process this information. SDDP has for many years been the most advantageous model for optimizing in a stochastic framework the operating of large multiple-reservoir systems. We present a variant of the traditional SDDP algorithm in which different exogenous hydrologic variables such as snow water equivalent and/or sea surface temperature can be included in the state space vector together with the past inflows. The incorporation of these exogenous variables relies on a built-in MPARX model to generate the inflows during both phases of the algorithm (backward optimization and forward simulation). The results are consistent with previous studies and show that good information about future flows can result in more efficient hydropower system operations. This paper demonstrates that the SDDP model can show operators how to achieve such gains in large hydropower systems.

Appendix A: SDDPX Parameter Estimation

The appendix shows how to analytically derive the parameters of the hyperplanes used to approximate the future benefit function in SDDPX. As indicated in section 2.2, the main modification lies in the calculation of the hyperplanes' parameters φ_{t+1}, χ_{t+1}, β_{t+1}, and Γ_{t+1} (see equation (5)). In particular, Γ_{t+1} which can be written as:

$$\begin{aligned}\Gamma_{t+1}h_{t+1}=&\gamma_{t+1,1}q_t+\gamma_{t+1,2}q_{t-1}+\ldots+\gamma_{t+1,p}q_{(t-p)+1}\\&+\gamma_{t+1,p+\kappa}X_{(t-\kappa)+1}+\ldots+\gamma_{t+1,p+b}X_{(t-b)+1}\end{aligned} \tag{A1}$$

According to the Karush-Kuhn-Tucker conditions for optimality, the derivative of the objective function with respect to the state variables S_i is given by:

$$\frac{\partial F}{\partial S_i} = -\sum \lambda_i \frac{\partial g_i}{\partial S_i} \tag{A2}$$

where λ_i is the dual information (Lagrange multiplier) of the convex optimization problem and g_i is the constraints (Kuhn & Tucker, 1951). Then, for the specific case at stage t and using constraints (4), (5), (8), and (10), the change of the one-stage objective function F_t respect to the state variables $s_t,\ w_t,\ h_t$, can be determined by:

$$\frac{\partial F_t}{\partial s_t} = \lambda_{w,t} + \sum_{h=1}^{H} \lambda_{hp,t}^{h} \psi_{t+1}^{h}/2 \tag{A3}$$

$$\frac{\partial F_t}{\partial w_t} = \lambda_{e,t} \tag{A4}$$

$$\frac{\partial F_t}{\partial h_t} = \lambda_{w,t} \frac{\partial q_t}{\partial h_t} + \sum_{l=1}^{L} \lambda_{c,t}^{l} \frac{\partial \left(\Gamma_{t+1}^{l} h_{t+1}\right)}{\partial h_t} \tag{A5}$$

where $\lambda_{w,t},\ \lambda_{e,t},\ \lambda_{c,t}^{l}$, and $\lambda_{hp,t}^{h}$ are, respectively, the vectors with the dual information associated to the mass balance (4), energy balance (10), the L cuts of the benefit-to-go function (5), and the H linear segments of the power functions (8).

Using (A1), we can calculate the derivatives in the above equation (A5) for each hydrologic variable $[q_{t-1},\ q_{t-2},\ldots,q_{t-p}, X_{t-1},\ X_{t-\kappa},\ldots, X_{t-b}]$:

$$\begin{aligned}
\frac{\partial(\Gamma_{t+1} h_{t+1})}{q_{t-1}} &= \gamma_{t+1,1}^{l} \frac{\partial q_t}{\partial q_{t-1}} + \gamma_{t+1,2}^{l} \\
\frac{\partial(\Gamma_{t+1} h_{t+1})}{q_{t-2}} &= \gamma_{t+1,1}^{l} \frac{\partial q_t}{\partial q_{t-2}} + \gamma_{t+1,3}^{l} \\
&\vdots \\
\frac{\partial(\Gamma_{t+1} h_{t+1})}{q_{t-p}} &= \gamma_{t+1,1}^{l} \frac{\partial q_t}{\partial q_{t-p}} \\
\frac{\partial(\Gamma_{t+1} h_{t+1})}{X_{t-\kappa}} &= \gamma_{t+1,1}^{l} \frac{\partial q_t}{\partial X_{t-\kappa}} + \gamma_{t+1,p+\kappa+1}^{l} \\
&\vdots \\
\frac{\partial(\Gamma_{t+1} h_{t+1})}{X_{t-b}} &= \gamma_{t+1,1}^{l} \frac{\partial q_t}{\partial X_{t-b}}
\end{aligned} \tag{A6}$$

Now, let us say that at stage t, s_t°, w_t°, and $h_t^{\circ} = [q_{t-1}^{\circ},\ q_{t-2}^{\circ}, \ldots,\ q_{t-p}^{\circ},\ X_{t-\kappa}^{\circ}, \ldots,\ X_{t-b}^{\circ}]$ are sampled and, in order to include the stochasticity of the problem, K vectors of inflows q_t^{K} are generated using the MPARX(p,b) (equation (12)). Since F_t^{k}, which will be added to the expected-benefit-to-go function at stage $(t-1)$, can be approximated by:

$$F_t^{k} \leq \varphi_t^{l,k} s_t^{\circ} + \chi_t^{l,k} w_t^{\circ} + \Gamma_t^{l,k} h_t^{\circ} + \beta_t^{l,k} \tag{A7}$$

the slopes $\varphi_t^{l,k}, \chi_t^{l,k}, \Gamma_t^{l,k} = [\gamma_{t,1}^{l,k}, \ldots, \gamma_{t,p}^{l,k}, \gamma_{t,p+\kappa}^{l,k}, \ldots, \gamma_{t,p+b}^{l,k}]$ are determined for each hydrologic scenario k using equations (A3), (A4), and (A6):

$$\frac{\partial F_t^{k}}{\partial s_t}(j) = \varphi_t^{l,k}(j) = \lambda_{w,t}^{k}(j) + \sum_{h=1}^{H} \lambda_{hp,t}^{h,k}(j) \psi_{t+1}^{h}(j)/2 \tag{A8}$$

$$\frac{\partial F_t^{k}}{\partial w_t}(c) = \chi_t^{l,k}(c) = \lambda_{e,t}^{k}(c) \tag{A9}$$

$$
\begin{aligned}
&\frac{\partial F_t^K}{\partial q_{t-1}}(j)=\gamma_{t,1}^{l,k}(j)=\left(\lambda_{w,t}^{l,k}(j)+\sum_{l=1}^{L}\lambda_{c,t}^{l,k}(j)\gamma_{t+1,1}^{l}(j)\right)\frac{\partial q_t}{\partial q_{t-1}}+\sum_{l=1}^{L}\lambda_{c,t}^{l,k}(j)\gamma_{t+1,2}^{l}(j)\\
&\frac{\partial F_t^K}{\partial q_{t-2}}(j)=\gamma_{t,2}^{l,k}(j)=\left(\lambda_{w,t}^{l,k}(j)+\sum_{l=1}^{L}\lambda_{c,t}^{l,k}(j)\gamma_{t+1,1}^{l}(j)\right)\frac{\partial q_t}{\partial q_{t-2}}+\sum_{l=1}^{L}\lambda_{c,t}^{l,k}(j)\gamma_{t+1,3}^{l}(j)\\
&\vdots\\
&\frac{\partial F_t^K}{\partial q_{t-p}}(j)=\gamma_{t,p}^{l,k}(j)=\left(\lambda_{w,t}^{l,k}(j)+\sum_{l=1}^{L}\lambda_{c,t}^{l,k}(j)\gamma_{t+1,1}^{l}(j)\right)\frac{\partial q_t}{\partial q_{t-p}}\\
&\frac{\partial F_t^K}{\partial X_{t-\kappa}}(j)=\gamma_{t,p+\kappa}^{l,k}(j)=\left(\lambda_{w,t}^{l,k}(j)+\sum_{l=1}^{L}\lambda_{c,t}^{l,k}(j)\gamma_{t+1,1}^{l}(j)\right)\frac{\partial q_t}{\partial X_{t-\kappa}}+\sum_{l=1}^{L}\lambda_{c,t}^{l,k}(j)\gamma_{t+1,p+\kappa+1}^{l}(j)\\
&\vdots\\
&\frac{\partial F_t^K}{\partial X_{t-b}}=\gamma_{t,p+b}^{l,k}(j)=\left(\lambda_{w,t}^{l,k}(j)+\sum_{l=1}^{L}\lambda_{c,t}^{l,k}(j)\gamma_{t+1,1}^{l}(j)\right)\frac{\partial q_t}{\partial X_{t-b}}
\end{aligned}
\tag{A10}
$$

Defining $\gamma(j)$ as:

$$
\gamma_t(j)=\lambda_{w,t}^{l,k}(j)+\sum_{l=1}^{L}\lambda_{c,t}^{l,k}(j)\gamma_{t+1,1}^{l}(j)
\tag{A11}
$$

and by using (12) to find the derivatives of q_t respect to the hydrologic variables, the set of equation (A10) can be rewritten as:

$$
\begin{aligned}
&\gamma_{t,1}^{l,k}(j)=\gamma_t(j)\frac{\sigma_{q_t}(j)}{\sigma_{q_{t-1}}(j)}\phi_{t,1}(j)+\sum_{l=1}^{L}\lambda_{c,t}^{l,k}(j)\gamma_{t+1,2}^{l}(j)\\
&\gamma_{t,2}^{l,k}(j)=\gamma_t(j)\frac{\sigma_{q_t}(j)}{\sigma_{q_{t-2}}(j)}\phi_{t,2}(j)+\sum_{l=1}^{L}\lambda_{c,t+1}^{l,k}(j)\gamma_{t+1,3}^{l}(j)\\
&\gamma_{t,p}^{l,k}(j)=\gamma_t(j)\frac{\sigma_{q_t}(j)}{\sigma_{q_{t-p}}(j)}\phi_{t,p}(j)\\
&\vdots\\
&\gamma_{t,p+\kappa}^{l,k}(j)=\gamma_t(j)\frac{\sigma_{X_t}(j)}{\sigma_{X_{t-\kappa}}(j)}\vartheta_{t,\kappa}(j)+\sum_{l=1}^{L}\lambda_{c,t+1}^{l,k}(j)\gamma_{t+1,p+\kappa+1}^{l}(j)\\
&\gamma_{t,p+b}^{l,k}(j)=\gamma_t(j)\frac{\sigma_{X_t}(j)}{\sigma_{X_{t-p}}(j)}\vartheta_{t,b}(j)
\end{aligned}
\tag{A12}
$$

Taking the expectation over the K artificially generated flows, the vector of slopes φ_t^l, $\chi_{t,1}^l$, $\gamma_{t,1}^l$, $\gamma_{t,2}^l, \ldots, \gamma_{t,p}^l$, $\gamma_{t,p+\kappa}^l, \ldots, \gamma_{t,p+b}^l$ can be determined:

$$
\varphi_t^l(j)=\frac{1}{K}\sum_{k=1}^{K}\varphi_t^{l,k}(j)
\tag{A13}
$$

$$
\chi_t^l(c)=\frac{1}{K}\sum_{k=1}^{K}\chi_t^{l,k}(c)
\tag{A14}
$$

$$
\gamma_{t,arx}^l(j)=\frac{1}{K}\sum_{k=1}^{K}\gamma_{t,arx}^{l,k}(j),
\tag{A15}
$$

$$
\forall arx=1,2,\ldots,p,p+\kappa,\ldots,p+b
$$

Finally, the constant term is given by:

$$\beta_t^l = \frac{1}{K}\sum_{k=1}^{K} F_t^k - \sum_J \varphi_t^l(j) s_t^\circ(j) - \sum_C \chi_t^l(c) w_t^\circ(c) \ldots$$
$$- \sum_J \gamma_{t,1}^l(j) q_{t-1}^\circ(j) - \sum_J \gamma_{t,2}^l(j) q_{t-2}^\circ(j) - \sum_J \gamma_{t,p}^l(j) q_{t-p}^\circ(j) \ldots \quad \text{(A16)}$$
$$- \sum_J \gamma_{t,p+\kappa}^l(j) X_{t-\kappa}^\circ(j) - \ldots - \sum_J \gamma_{t,p+b}^l(j) X_{t-b}^\circ(j)$$

Acknowledgments
Authors acknowledge the CRDPJ project funded by NSERC and Rio Tinto Alcan, and NSERC Strategic Network Project FloodNet. We also thank the reviewers for their constructive comments and suggestions. We thank Dr. Charles Rougé and Dr. Sara Séguin for their valuable discussions. Supporting data are not publicly available and belong to Rio Tinto, the private company operating the power system used to illustrate the proposed methodology. These data can be requested by contacting the third author (pascal.cote@riotinto.com).

References

Ahmad, A., El-Shafie, A., Razali, S. F. M., & Mohamad, Z. S. (2014). Reservoir optimization in water resources: A review. *Water Resource Management*, *28*(11), 3391–3405. https://doi.org/10.1007/s11269-014-0700-5

Archibald, T. W., Buchanan, C. S., McKinnon, K. I. M., & Thomas, L. C. (1999). Nested Benders decomposition and dynamic programming for reservoir optimisation. *Journal of the Operational Research Society*, *50*(5), 468–479. https://doi.org/10.1057/palgrave.jors.2600727

Bellman, R. (1957). *Dynamic programming* (1 ed.). Princeton, NJ: Princeton University Press.

Bras, R., Buchanan, R., & Curry, K. (1983). Real time adaptive closed loop control of reservoirs with the High Aswan Dam as a case study. *Water Resources Research*, *19*(1), 33–52. https://doi.org/10.1029/WR019i001p00033

Cerisola, S., Latorre, J. M., & Ramos, A. (2012). Stochastic dual dynamic programming applied to nonconvex hydrothermal models. *European Journal of Operational Research*, *218*(3), 687–697. https://doi.org/10.1016/j.ejor.2011.11.040

Côté, P., Haguma, D., Leconte, R., & Krau, S. (2011). Stochastic optimisation of Hydro Quebec hydropower installations: A statistical comparison between SDP and SSDP methods. *Canadian Journal of Civil Engineering*, *1434*(April), 1427–1434. https://doi.org/10.1139/l11-101

Desreumaux, Q., Côté, P., & Leconte, R. (2014). Role of hydrologic information in stochastic dynamic programming: A case study of the Kemano hydropower system in British Columbia. *Canadian Journal of Civil Engineering*, *41*(9), 839–844. https://doi.org/10.1139/cjce-2013-0370

Faber, B., & Stedinger, J. (2001). Reservoir optimization using sampling SDP with ensemble streamflow prediction (ESP) forecasts. *Journal of Hydrology*, *249*, 1113–1133. https://doi.org/10.1016/S0022-1694(01)00419-X

Gelati, E., Madsen, H., & Rosbjerg, D. (2013). Reservoir operation using El Niño forecasts case study of Daule Peripa and Baba, Ecuador. *Hydrological Sciences Journal*, *59*(8), 1559–1581. https://doi.org/10.1080/02626667.2013.831978

Gjelsvik, A., Mo, B., & Haugstad, A. (2010). Long and medium term operations planning and stochastic modelling in hydro-dominated power systems based on stochastic dual dynamic programming. In S. Rebennack et al. (Eds.), *Handbook of power systems I, Energy systems* (pp. 33–55). Berlin, Heidelberg: Springer. https://doi.org/10.1007/978-3-642-02493-1

Goor, Q., Kelman, R., & Tilmant, A. (2011). Optimal multipurpose multireservoir operation model with variable productivity of hydropower plants. *Journal of Water Resources Planning and Management*, *137*(3), 258–267. https://doi.org/10.1061/(ASCE)WR.1943-5452

Hamlet, A. F., & Lettenmaier, D. P. (1999). Columbia River streamflow forecasting based on ENSO and PDO climate signals. *Journal of Water Resources Planning and Management*, *125*(6), 333–341.

Homen-de Mello, T., de Matos, V. L., & Finardi, E. C. (2011). Sampling strategies and stopping criteria for stochastic dual dynamic programming: A case study in long term hydrothermal scheduling. *Energy Systems*, *2*(1), 1–31. https://doi.org/10.1007/s12667-011-0024-y

Karamouz, M., & Vasiliadis, H. V. (1992). Bayesian stochastic optimization of reservoir operation using uncertain forecasts. *Water Resources Research*, *28*(5), 1221–1232. https://doi.org/10.1029/92WR00103

Kelman, J., Stedinger, J., Cooper, L., Hsu, E., & Yuan, S. (1990). Sampling stochastic dynamic programming applied to reservoir operation. *Water Resources Research*, *26*(3), 447–454. https://doi.org/10.1029/WR026i003p00447

Kim, Y., & Palmer, R. (1997). Value of seasonal flow forecasts in Bayesian stochastic programming. *Journal of Water Resources Planning and Management*, *123*(6), 327–335. https://doi.org/10.1061/(ASCE)0733-9496(1997)123:6(327)

Kim, Y-O., Eum, H., Lee, E., & Ko, I. (2007). Optimizing operational policies of a Korean multireservoir system using sampling stochastic dynamic programming with ensemble streamflow prediction. *Journal of Water Resources Planning and Management*, *133*(1), 4–14.

Kristiansen, T. (2004). Financial risk management in the electric power industry using stochastic optimization. *Advanced Modelling and Optimization*, *6*(2), 17–24.

Kuhn, H. W., & Tucker, A. W. (1951). Nonlinear programming. In *Proceedings of the second Berkeley symposium on mathematical statistics and probability* (pp. 481–492). Berkeley, CA: University of California Press.

Kwon, H.-H., Brown, C., Xu, K., & Lall, U. (2009). Seasonal and annual maximum streamflow forecasting using climate information: Application to the Three Gorges Dam in the Yangtze River basin, *Hydrological Sciences Journal*, *54*(3), 582–595. https://doi.org/10.1623/hysj.54.3.582

Labadie, J. W. (2004). Optimal operation of multireservoir systems: State-of-the-art review. *Journal of Water Resources Planning and Management*, *130*(2), 93–111. https://doi.org/10.1061/(ASCE)0733-9496(2004)130:2(93)

Ljung, L. (1999). *System identification: Theory for the user*. Englewood Cliffs, NJ: Prentice-Hall.

Lohmann, T., Hering, A. S., & Rebennack, S. (2015). Spatio-temporal hydro forecasting of multireservoir inflows for hydro-thermal scheduling. *European Journal of Operational Research*, *255*(1), 243–258. https://doi.org/10.1016/j.ejor.2016.05.011

Macian-Sorribes, H., Tilmant, A., & Pulido-Velazquez, M. (2016). Improving operating policies of large-scale surface-groundwater systems through stochastic programming. *Water Resources Research*, *53*, 1407–1423. https://doi.org/10.1002/2016WR019573

Matos, V. L. D., & Finardi, E. C. (2012). A computational study of a stochastic optimization model for long term hydrothermal scheduling. *International Journal of Electrical Power & Energy Systems*, *43*(1), 1443–1452. https://doi.org/10.1016/j.ijepes.2012.06.021

Mo, B., Gjelsvik, A., & Grundt, A. (2001). Integrated risk management of hydro power scheduling and contract management. *IEEE Transactions on Power Systems*, *16*(2), 216–221. https://doi.org/10.1109/59.918289

New York Independent System Operator (NYISO) (2017). Hourly custom report-Time-Weighted/Integrated Real-Time LBMP-Reference Bus. Rensselaer, NY: New York Independent System Operator. Retrieved fromhttp://www.nyiso.com

Oliveira, R., & Loucks, D. P. (1997). Operating rules for multireservoir systems. *Water Resources Research*, *33*(4), 839–852. https://doi.org/10.1029/96WR03745

Pereira, M. (1989). Optimal stochastic operations scheduling of large hydroelectric systems. *International Journal of Electrical Power & Energy Systems*, *11*(3), 161–169. https://doi.org/10.1016/0142-0615(89)90025-2

Pereira, M. V. F., & Pinto, L. M. V. G. (1991). Multi-stage stochastic optimization applied to energy planning. *Mathematical Programming*, *52*(1–3), 359–375. https://doi.org/10.1007/BF01582895

Pereira-Cardenal, S. J., Mo, B., Gjelsvik, A., Riegels, N. D., Arnbjerg-Nielsen, K., & Bauer-Gottwein, P. (2016). Joint optimization of regional water-power systems. *Advances in Water Resources*, *92*, 200–207. https://doi.org/10.1016/j.advwatres.2016.04.004

Pina, J., Tilmant, A., & Anctil, F. (2016). Horizontal approach to assess the impact of climate change on water resources systems. *Journal of Water Resources Planning and Management*, *143*, 04016081-1. https://doi.org/10.1061/(ASCE)WR.1943-5452.0000737

Poorsepahy-Samian, H., Espanmanesh, V., & Zahraie, B. (2016). Improved inflow modeling in stochastic dual dynamic programming. *Journal of Water Resources Planning and Management*, *142*, 04016065-1. https://doi.org/10.1061/(ASCE)WR.1943-5452.0000713

Pritchard, G. (2015). Stochastic inflow modeling for hydropower scheduling problems. *European Journal of Operational Research*, *246*, 496–504. https://doi.org/10.1016/j.ejor.2015.05.022

Rani, D., & Moreira, M. M. (2009). Simulation optimization modeling: A survey and potential application in reservoir systems operation. *Water Resource Management*, *24*(6), 1107–1138. https://doi.org/10.1007/s11269-009-9488-0

Raso, L., Malaterre, P. O., & Bader, J. C. (2017). Effective streamflow process modeling for optimal reservoir operation using stochastic dual dynamic programming. *Journal of Water Resources Planning and Management*, *143*, 04017003-1. https://doi.org/10.1061/(ASCE)WR.1943-5452.0000746

Rotting, T., & Gjelsvik, A. (1992). Stochastic dual dynamic programming for seasonal scheduling in the Norwegian power system. *IEEE Transactions on Power Systems*, *7*(1), 273–279. https://doi.org/10.1109/59.141714

Shapiro, A., Tekaya, W., da Costa, J. P., & Soares, M. P. (2013). Risk neutral and risk averse Stochastic Dual Dynamic Programming method. *European Journal of Operational Research*, *224*(2), 375–391. https://doi.org/10.1016/j.ejor.2012.08.022

Stedinger, J. R., Sule, B. F., & Loucks, D. P. (1984). Stochastic dynamic programming models for reservoir operation optimization. *Water Resources Research*, *20*(11), 1499–1505. https://doi.org/10.1029/WR020i011p01499

Tejada-Guibert, J. A., Johnson, S. A., & Stedinger, J. R. (1995). The value of hydrologic information in stochastic dynamic programming models of a multireservoir system. *Water Resources Research*, *31*(10), 2571–2579. https://doi.org/10.1029/95WR02172

Tilmant, A., & Kelman, R. (2007). A stochastic approach to analyze trade-offs and risks associated with large-scale water resources systems. *Water Resources Research*, *43*, W06425. https://doi.org/10.1029/2006WR005094

Tilmant, A., & Kinzelbach, W. (2012). The cost of noncooperation in international river basins. *Water Resources Research*, *48*, W01503. https://doi.org/10.1029/2011WR011034

Tilmant, A., Pinte, D., & Goor, Q. (2008). Assessing marginal water values in multipurpose multireservoir systems via stochastic programming. *Water Resources Research*, *44*, W12431. https://doi.org/10.1029/2008WR007024

Yeh, W. W.-G. (1985). Reservoir management and operations models: A state-of-the-art review. *Water Resources Research*, *21*(12), 1797–1818. https://doi.org/10.1029/WR021i012p01797

Zahraie, B., & Karamouz, M. (2004). Hydropower reservoirs operation: A time decomposition approach. *Scientia Iranica*, *11*(1–2), 92–103.

Zhao, T., Zhao, J., & Yang, D. (2014). Improved dynamic programming for hydropower reservoir operation. *Journal of Water Resources Planning and Management*, *140*(March), 365–374. https://doi.org/10.1061/(ASCE)WR1943-5452.0000343